Eur. Phys. J. D **9**, 351–354 (1999)

THE EUROPEAN PHYSICAL JOURNAL D

EDP Sciences

Thermionic emission laser spectroscopy of stored C_{60}^-

K. Hansen[1], J.U. Andersen[1], H. Cederquist[2], C. Gottrup[1], P. Hvelplund[1], M.O. Larsson[1,a], V.V. Petrunin[1], and H.T. Schmidt[2]

[1] Institute of Physics and Astronomy, University of Aarhus, Ny Munkegade, Bygn. 520, DK-8000 Aarhus C, Denmark
[2] Atomic Physics, Stockholm University, Stockholm, Sweden

Received: 31 August 1998 / Received in final form: 14 January 1999

Abstract. Thermal emission of electrons from clusters is enhanced after the absorption of photons. We have used this process to measure the photoabsorption cross sections of hot C_{60} anions in the visible and near-infrared part of the spectrum, using the ion storage ring ASTRID (Aarhus STorage RIng, Denmark).

PACS. 78.40.R Absorption spectra of fullerenes – 42.62.F Laser spectroscopy – 79.40 Thermionic emission

1 Introduction

Optical spectroscopy of free fullerenes has, with a few exceptions [1–4], been limited to the spectroscopy of vapour [5, 6] or pseudofree molecules in noble gas matrices or droplets [7–10]. On one hand, the low vapor pressure makes the traditional absorption spectroscopy of cold fullerenes extremely difficult. On the other hand, the combination of a large number of degrees of freedom and a binding energy which is high compared to the photon energies of interest precludes the traditional depletion spectroscopy that has been applied succesfully in other cases (see examples in [11]).

The situation for the ionic species is potentially worse, since not even vapour absorption spectroscopy is feasible. However, for the negatively charged fullenes, the relatively small electron affinity opens a route to optical spectroscopy of a mass- and charge-selected molecular beam. In this contribution we will describe how this idea has been implemented in an experiment at the storage ring ASTRID (Aarhus STorage RIng, Denmark). The facility has previously been used for the storage of fullerene and metal cluster anions and for the monitoring of their spontaneous decay through thermionic emission [12–14]. The fullerenes were found to decay with a power law time dependence at short times and a modified exponential decay at longer times. This behaviour could be modeled if one takes into account the unimolecular radiative cooling from the highly excited molecules, similar to what was found earlier for the positively charged, smaller fullerenes [15].

This behaviour is the consequence of the properties of the ensemble that describes the cooling molecules, and it can be used to extract, in a quantitative way, the photoabsorption cross sections from measurements of photo-induced enhancement of thermionic emission. We will briefly describe the experiment and results and then concentrate on the method used to extract information from the data. A more detailed account of the results will be published elsewhere.

2 Experiment

The fullerene ions were produced in a plasma ion source and injected into the ring a few hundred microseconds after their creation in the source. During the 100 ms storage period, the anions emitted electrons spontaneously, with a rapidly decreasing rate, as described in [13]. The signal measured was the number of neutral molecules hitting the detector at one corner of ASTRID; this number represents the integrated rate of electron emission during flight through one side of the storage ring (about 80 μs). At a preselected time, a quarter of the ion beam was irradiated with a short ($\approx$ 10 ns) pulse from a tuneable 10 Hz Nd:YAG-pumped OPO laser. The energy absorbed from the laser pulse heated the molecules and increased the rate of the thermally activated electron emission. The increased rate was measured with a delay determined by the geometry to be one half turn plus a multiple of turns, or 180 μs + $n \times$ 360 μs. Since the laser and ion beams overlapped on only one side of the ring, the spectrum simultaneously recorded the enhanced signal due to photoabsorption and the base signal. The acquisition channel width was chosen to be 30 μs so that one turn in the ring corresponded to 12 channels. The enhanced signal was present in 2–3 of these, or close to a quarter of one full turn, indicating a good laser beam/ion beam overlap. The rest of the channels provided the reference. The enhanced thermionic emission measured this way depends on the optical absorption cross section, the photon energy, and the internal energy of the ion.

[a] *Present address*: Department of Physical Chemistry, Uppsala University, S-75121 Uppsala, Sweden

The laser was triggered at various times between 0.5 and 80 ms after ion injection and the photon energy was varied between 0.95 and 2.9 eV (425–1300 nm). According to the modeling in [13], this time range corresponds to a temperature of spontaneously decaying molecules that varies by more than 20% (from 1500 K to 1150 K) by the combined effect of cooling by depletion of the hottest molecules and radiative energy loss. For each laser firing time, the wavelength was scanned in steps of typically 25 nm for the visible and 50 nm for the IR region, except for a few spectra that were scanned much denser, about 1 nm, in the IR region.

The laser pulse energies were measured at the exit window of the storage ring. The beam position was stable, and the optics was designed to minimize changes in the position and width of the laser beam during wavelength scans. The overlap of the two beams should therefore have been nearly constant, with only a slow variation with wavelength. However, there was a large uncertainty in the magnitude of the overlap.

The linearity of the absorption was checked at two wavelengths by attenuation of the laser fluence by neutral density filters. The enhancement versus pulse energy showed a small positive curvature, indicating that a small number of molecules absorbed a second photon. Since the laser pulse lasted 10 ns, two- or multi-photon absorption processes were not likely to occur. Multiple photon absorption was therefore sequential, so we need to use Poissson statistics for the number of absorbed photons. This will be taken into account in the data analysis.

3 Results

Figure 1 shows a spectrum recorded at a 7.1 ms delay between ion beam injection and laser triggering. Figure 1(a) gives an overview of the decay from a few hundred μs after injection to 100 ms. The rapid decrease in the signal and the nonexponential nature of the decay is seen clearly from this figure. The interpretation of this curve in terms of radiative cooling and proper ensemble averaging is discussed in [13]. At 7.1 ms, the decay component due to photon absorption appears abruptly, but as a barely visible signal superposed on the spontaneous decay. Figure 1(b) shows an expanded view of the same spectrum around the laser firing time. The enhanced decay for a few channels in each bunch after the laser pulse is seen much more clearly here than in Fig. 1(a).

Quantitatively, the enhancement R is defined as the increase in signal relative to the spontaneous decay, which is easily extracted from the spectrum. For this purpose we have assumed that the enhanced signal appears in one channel in the spectrum. For any given photon energy, the enhancement was smallest for the shortest delay times, i.e., for the hottest molecules. At longer times, it was up to 100 times larger. For short delay times, it disappeared quickly, whereas for longer delay times it could persist for many turns.

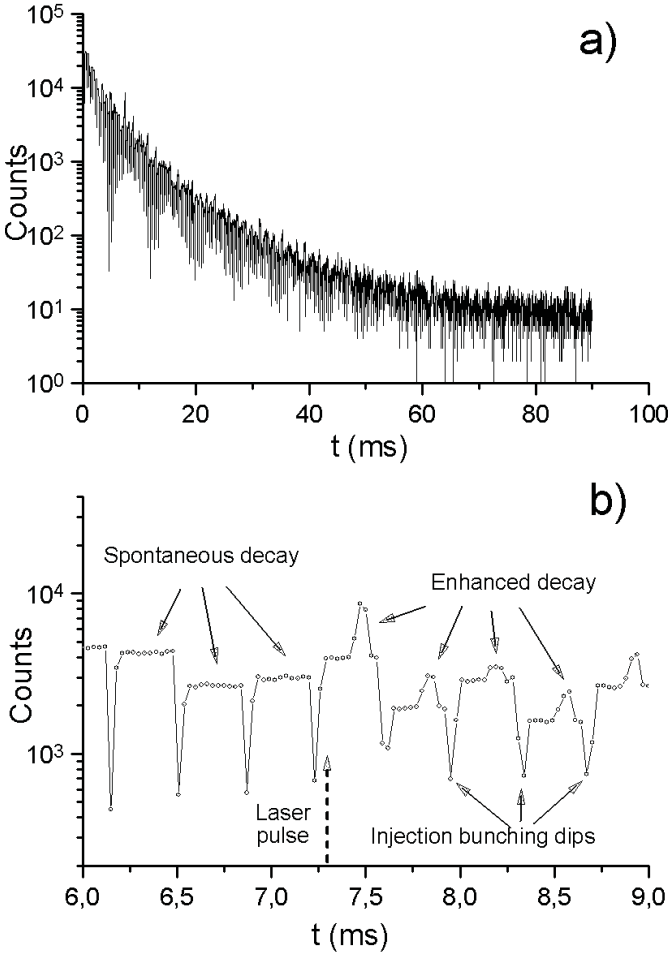

Fig. 1. The electron emission signal for a laser pulse fired with a nominal delay of 7.1 ms after injection of the molecules into the ring. Apart from the weak signal at 7–8 ms, the curve in (a) is identical to the one obtained for spontaneously decaying fullerenes. The periodic dips in count rate are due to the less-than-complete filling of the ring during injection with ions and occur periodically with the circulation period of 360 μs. In (b) the enhanced decay is seen more clearly. The fluctuations of the signal with rotation period is due to betatron oscillations in the ion beam. Besides the laser beam geometry, this is the main problem for absolute cross-section measurements with this method.

The enhancement varied smoothly with photon energy, with no sign of sharp peaks in either the visible or the infrared region. The maximum photon energy is below the lowest strong absorption peak for a vapor of neutral C_{60} [5, 6], and from the blue part of the visible spectrum towards the red, the enhancement signal decreased monotonically. In the infrared region, on the other hand, we found a broad absorption peak around 1.2 eV. This position is expected from the analogous absorption spectra of C_{60}^- in solution [16]. The width of the peak is a few hundred nm and it is likely to contain vibronic transitions. However, no fine structure could be resolved in the peaks. These features were persistent, irrespective of the delay between injection and laser pulse.

4 Data analysis and discussion

The (dimensionless) enhancement signal R depends on five quantities: The cross section for absorption, the laser fluence, the photon energy, the time of absorption, and the time lag between absorption and measurement. In order to relate the enhancement to these quantities and to extract the cross sections from the data, it is essential that one take into account the nonexponential nature of the decay. The source yields molecules with a smooth energy distribution, which, together with radiative cooling, determines the precise decay curve [13]. Immediately before photon absorption, the emission rate is given by

$$I(t) = \int_0^\infty \varrho(E,t)k(E)\ \mathrm{d}E \tag{1}$$

where t is the time that elapses after the molecule leaves the source. The energy distribution $\varrho(E,t)$ depends on time through radiative cooling and through depletion by decay of the hottest molecules. The energy distribution has a well-defined edge at a time-dependent energy $E_0(t)$.

Only molecules with internal energy close to E_0 contribute to the yield; the distribution can therefore be approximated by a constant in the region of interest,

$$I(t) = c\int_0^{E_0(t)} k(E)\ \mathrm{d}E. \tag{2}$$

Absorption of a single photon shifts the edge upwards by the photon energy for a fraction of the molecules which is given by the product of cross section and laser fluence, σF. After single-photon absorption, the measured rate is

$$I(t)_{\hbar\omega} = c\int_0^{E_0(t)} k(E)\ \mathrm{d}E + \sigma F\, c\int_{E_0(t)}^{E_0(t)+\hbar\omega} k(E)\mathrm{d}E. \tag{3}$$

The relative increase in the signal, the enhancement, is then

$$R_1(\sigma,\hbar\omega,t,t) = \frac{I(t)_{\hbar\omega} - I(t)}{I(t)} = \frac{\sigma F\ \int_{E_0(t)}^{E_0(t)+\hbar\omega} k(E)\mathrm{d}E}{\int_0^{E_0(t)} k(E)\ \mathrm{d}E}. \tag{4}$$

The subscript of R indicates single-photon absorption. This result corresponds to instantaneous observation. With a time lag between laser pulse and measurement, the enhancement is reduced through the partial decay of the shifted part of the energy distribution:

$$R_1(\sigma,\hbar\omega,t,t+t_1) = \frac{\sigma F\ \int_{E_0(t)}^{E_0(t)+\hbar\omega} k(E)e^{-k(E)t_1}\,\mathrm{d}E}{\int_0^{E_0(t+t_1)} k(E)\ \mathrm{d}E}. \tag{5}$$

The time lag t_1 is so short that radiative cooling can be ignored between photon absorption and detection ($t_1 < \tau$ where $\tau = 4.3\,\mathrm{ms}$ is the characteristic radiation time for C_{60} [13]). The integrals can be performed with the substitution

$$\frac{\mathrm{d}k}{k\,\mathrm{d}E} \approx \frac{G^2}{CE_\mathrm{b}} \approx 1.4\,\mathrm{eV}^{-1}. \tag{6}$$

Here $E_\mathrm{b} = 2.65\,\mathrm{eV}$ is the electron binding and $C = 160$ is the heat capacity, while $G \equiv log(\omega_\mathrm{e}\tau) = 24.1$ is the Gspann parameter for $t = \tau$, defined with the frequency factor ω_e from the electron emission rate constant $k = \omega_\mathrm{e}\exp(-E_\mathrm{b}/T)$ [13]. The energy dependence of $\mathrm{d}k/k\,\mathrm{d}E$ is weak and we will use the constant value given above. The result is

$$R_1(\sigma,\hbar\omega,t,t+t_1) = \frac{\sigma F\left(e^{-k(E_0(t))t_1} - e^{-(k(E_0(t))+\hbar\omega)t_1}\right)}{t_1\ k(E_0(t+t_1))}, \tag{7}$$

where

$$k(E_0(t)+\hbar\omega)\ =\ k(E_0)\ e^{\hbar\omega 1.4\ \mathrm{eV}^{-1}}. \tag{8}$$

The variation of $k(E_0(t)))$ with time was found in [13] to be

$$k(E_0(t)) = \frac{1}{\tau}\frac{\left(1+\frac{t\ (n-1)}{\tau\ G}\right)^{\frac{-2}{n-1}}}{\exp\left(G\left(1+\frac{t\ (n-1)}{\tau\ G}\right)^{\frac{1}{n-1}} - G\right) - 1}, \tag{9}$$

with the value of τ and G given above and with $n = 7.6$. The normalization has been determined by extrapolation to short times where $k(E_0(t)) = 1/t$. The delayed signal in (7) depends on the exponential decay between t and t_1 of the high-energy population and on the radiative cooling (9).

For the nonradiative case where $E_0(t)$ is determined through $k(E_0) = 1/t$, the result reduces to

$$R_1(\sigma,\hbar\omega,t,t+t_1) = \sigma F\ (t/t_1+1)\left(e^{-t_1/t} - e^{-t_1 k(E_0+\hbar\omega)}\right). \tag{10}$$

The expression in (7) can be fitted for the only unknown parameter, the cross section σ. However, since the enhancement depends strongly on the amount of energy absorbed, we must take multi-photon absorption into account, even though the average number of photons absorbed is normally low. This is done by summing over a Poisson statistics for photon number absorption and inserting the proper multiple of the photon energy into the expression above,

$$R_n(\sigma,\hbar\omega,t,t+t_1) = \frac{(\sigma F)^n e^{-\sigma F}}{n!} \times \frac{\left(e^{-k(E_0(t))t_1} - e^{-(k(E_0(t))+n\hbar\omega)t_1}\right)}{t_1\ k(E_0(t+t_1))}. \tag{11}$$

The total enhancement is then

$$R = \sum_{n=1}^{\infty} R_n. \tag{12}$$

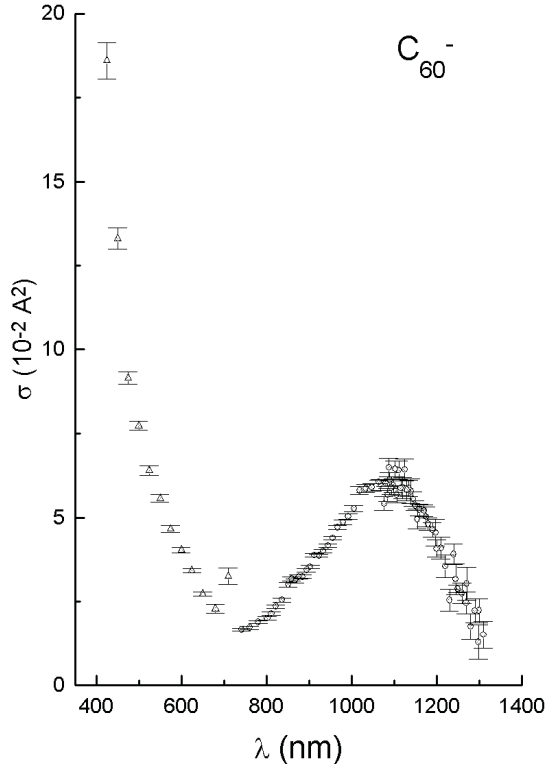

Fig. 2. The C_{60}^- absorption spectrum in the visible and near infrared region at $T = 1400$ K. The two parts are recorded at slightly different cooling times, i.e., delays between injection and laser pulse (5 and 7 μs), for intensity reasons. The spectrum is extracted from the raw data using the formula derived here, (11), (12), with one overall adjustment of the absolute scale as described in the text. Uncertainties are statistical only. True values are estimated to be within a factor 2 of the ones shown.

This is used to fit the value of the absorption probability σF numerically. Although inclusion of multi-photon absorption changes the estimate of the absolute magnitude of the cross section and is important for the reproduction of the fluence dependence of the signal, the relative cross sections do not change much from the ones resulting from the approximation of the absorption by one-photon absorption alone. From the fit of σF, the cross sections are found by normalization with the number of photons per pulse.

The cross section is shown in Fig. 2. The spectrum consists of a smooth but strong decrease towards longer wavelengths, interrupted by a broad but still well-defined peak around 1050 nm, or 1.2 eV. The peak is fairly broad, and at least part of the width has its origin in the envelope of the sidebands and hot bands flanking the central transition.

The measured cross section was integrated over the 1064 nm/1.17 eV peak and the integral compared with the oscillator strength of the transition in solution spectra [16]. The latter is 0.027 eV Å^2. Using the laser fluence from the exit window of the ring, our absolute cross section is higher by a factor of 10. This computation underestimates the photon flux at the interaction point by an unknown but significant factor, typically $\sim$4. Betatron oscillations introduce a similar error. We conclude that our measured infrared cross sections are consistent with the oscillator strength of C_{60}^- in solution, and we have used these to normalize the overall scale in Fig. 2.

5 Summary

We have applied a novel technique to measure the photoabsorption cross sections of highly excited C_{60}^- in the ion storage ring ASTRID. The experimental signal for absorption has been related quantitatively to the cross section through application of the appropriate ensemble for modeling the thermionic emission process and the internal energy contents of the molecules.

This work was supported by the Danish National Research Foundation through the research center ACAP.

References

1. R.E. Haufler, Y. Chai, L.P.F. Chibante, M.R. Fraelich, R.B. Weisman, R.F. Curl, R.E. Smalley: J. Chem. Phys. **95**, 2197 (1991)
2. K. Hansen, R. Müller, P. Brockhaus, E.E.B. Campbell, I.V. Hertel: Z. Phys. D **42**, 153 (1997)
3. J. de Vries, H. Steger, B. Kamke, C. Menzel, B. Weisser, W. Kamke, I.V. Hertel: Chem. Phys. Lett. **188**, 159 (1992)
4. H. Steger, J. de Vries, B. Kamke. W. Kamke, T. Drewello: Chem. Phys. Lett. **194**, 452 (1992)
5. C.E. Coheur, M. Carleer, R. Colin: J. Phys. B **29**, 4987 (1996)
6. A.L. Smith: J. Phys. B **29**, 4975 (1996)
7. J.D. Close, F. Federmann, K. Hoffmann, N. Quaas: Chem. Phys. Lett. **276**, 393 (1997)
8. J. Fulara, M. Jakobi, J. Maier: Chem. Phys. Lett. **211**, 227 (1993)
9. A. Sassara, G. Zerza, M. Chergui: J. Phys. B **29**, 4997 (1996)
10. A.N. Starukhin *et al.*: J. Lumin. **72**–**74**, 457 (1997)
11. W.A. de Heer: Rev. Mod. Phys. **65**, 611 (1993)
12. C. Brink, L.H. Andersen, P. Hvelplund, D. Mathur, J.D. Voldstad: Chem. Phys. Lett. **233**, 52 (1995)
13. J.U. Andersen, C. Brink, P. Hvelplund, M.O. Larsson, B. Bech Nielsen, H. Shen: Phys. Rev. Lett. **77**, 3991 (1996)
14. J.U. Andersen *et al.*: Z. Phys. D **40**, 365 (1997)
15. K. Hansen, E.E.B. Campbell: J. Chem. Phys. **104**, 5012 (1996)
16. D.R. Lawson, D.L. Feldheim, C.A. Foss, P.K. Dorhout, C.M. Elliott, C.R. Martin, B. Parkinson: J. Electrochem. Soc. **139**, L68 (1992)